EARTHQUAKE ENGINEERING AND STRUCTURAL DYNAMICS
Earthquake Engng. Struct. Dyn. **28**, 957–977 (1999)

DETERMINATION OF DUCTILITY FACTOR CONSIDERING DIFFERENT HYSTERETIC MODELS

LI HYUNG LEE[1,*,†], SANG WHAN HAN[1,†] AND YOUNG HUN OH[2,‡]
[1]*Department of Architectural Engineering, Hanyang University, Seoul, South Korea*
[2]*Advanced Structure Research Station, Hanyang University, Seoul, South Korea*

SUMMARY

In current seismic design procedures, base shear is calculated by the elastic strength demand divided by the strength reduction factor. This factor is well known as the response modification factor, R, which accounts for ductility, overstrength, redundancy, and damping of a structural system. In this study, the R factor accounting for ductility is called the 'ductility factor', R_μ. The R_μ factor is defined as the ratio of elastic strength demand imposed on the SDOF system to inelastic strength demand for a given ductility ratio. The R_μ factor allows a system to behave inelastically within the target ductility ratio during the design level earthquake ground motion. The objective of this study is to determine the ductility factor considering different hysteretic models. It usually requires large computational efforts to determine the R_μ factor. In order to reduce the computational efforts, the R_μ factor is prepared as a functional form in this study. For this purpose, statistical studies are carried out using forty different earthquake ground motions recorded at a stiff soil site. The R_μ factor is assumed to be a function of the characteristic parameters of each hysteretic model, target ductility ratio and structural period. The effects of each hysteretic model to the R_μ factor are also discussed. Copyright © 1999 John Wiley & Sons, Ltd.

KEY WORDS: seismic design; strength reduction factor; ductility factor (R_μ); target ductility ratio; hysteretic models

1. INTRODUCTION

Most seismic design provisions allow structures to behave inelastically during a severe Earth-Quake Ground Motion (EQGM). For this reason, the required elastic strength demand is reduced by a scaling factor which is known as either a strength reduction factor or a response modification factor, R. This factor accounts for ductility, overstrength, damping and redundancy inherent in a structure. Strength reduction factor, R, has been determined mainly based on engineering judgement and accumulated experiences from the past earthquakes rather than theoretical background. Even if knowledge and lessons have been gained from past earthquakes,

* Correspondence to: Li Hyung Lee, Department of Architectural Engineering, Hanyang University, 17 Haengdang-dong, Songdong-ku, Seoul 133-791, Korea. E-mail: swhan@email.hanyang.ac.kr
† Professor, Ph.D.
‡ Researcher, Ph.D.
Contract/grant sponsor: STRESS

CCC 0098–8847/99/090957–21$17·50

Received 21 September 1998
Revised 12 February 1999

this factor has not been changed or reviewed substantively since horizontal force factor, K, was introduced by the SEAOC "Blue Book" in 1959.

According to the research results in recent years, the assigned values for the R factor has been questioned.[1,2] (ATC-19 and ATC-34). Also the use of a single value for the R factor for a given structural system becomes doubtable. As a draft form in ATC-19 and ATC-34, the R factor is split into three factors in order to account for the effect of ductility, damping, redundancy and overstrength, explicitly.

One of the earliest and better known studies on strength reduction factors is that of Newmark and Hall.[3] They studied elastic and inelastic response spectra of a 5 per cent damped SDOF system subjected to three recorded ground motions and pulse-type excitations. Based on statistical studies, they proposed strength reduction factor, R, as a functional form which allows the construction of the inelastic response spectra from the elastic response spectra. The type of a functional form is dependent on the region of the natural period of a structure. Riddell and Newmark[4] performed statistical studies for evaluating the R_μ factor using 10 different earthquake ground motions recorded in the rock and alluvium soil condition. They considered three different hysteretic models such as the elasto-perfectly plastic, bilinear and stiffness degradation models. According to their studies, the elasto-perfectly plastic model gives a conservative R_μ factor. Nassar and Krawinkler[5] evaluated mean strength reduction factors of bilinear and stiffness degrading systems subjected to 15 ground motions recorded on firm soil sites in the western United States. They proposed a functional form of the R factor with respect to ductility, the natural period and the second slope of the bilinear model. Miranda[6] performed studies similar to that of Nassar and Krawinkler[3]. He used more earthquake records and considered the effect of different soil conditions. Nassar and Krawinkler[5] and Miranda[6] studied the influence of earthquake magnitude and epicentral distance on the R_μ factors. Both studies concluded that the effects of both parameters are negligible on the R_μ factor. Han and Wen[7] proposed the R_μ factor for a special moment resisting steel frame (SMRSF) based on statistical studies.

This study establishes the functional form of ductility factor, R_μ, which is able to account for the characteristic of different hysteretic models. For this purpose, statistical studies are carried out. Forty earthquake ground motion records are used for this study. Five different hysteretic models are considered, such as the elasto-perfectly plastic, bilinear, strength degradation, stiffness degradation and pinching models.

2. EVALUATION OF DUCTILITY FACTOR, R_μ

Under a given earthquake ground motion the inelastic deformation of a system generally increases as its yield strength level becomes lower. Ductility factor, R_μ is defined as the ratio of the elastic strength demand $F_y(\mu = 1)$ to the inelastic yield strength demand $F_y(\mu_t)$ for a given target ductility ratio (μ_t), which is represented by the following equation:

$$R_\mu = \frac{F_y(\mu = 1)}{F_y(\mu = \mu_t)} \tag{1}$$

The relationship between $F_y(\mu = 1)$ and $F_y(\mu = \mu_t)$ is shown in Figure 1. The iterative procedure is required for calibrating the R_μ factor to attain a given target ductility ratio, μ_t. The process is shown in Figure 2. However, the ductility ratio, μ may not always increase monotonically as the

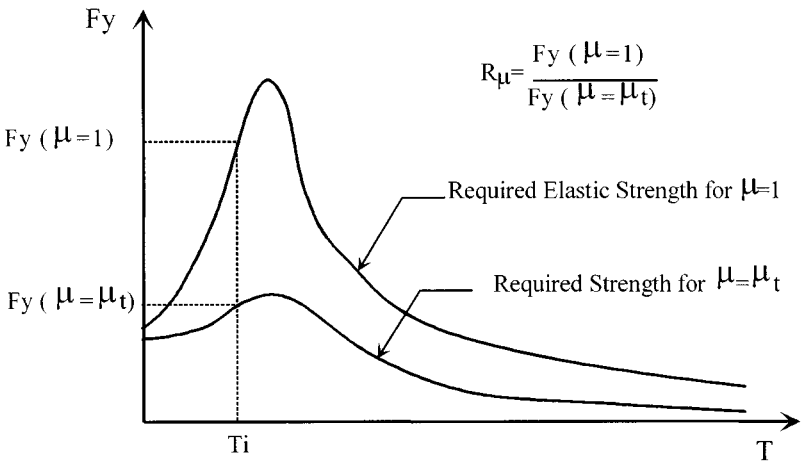

Figure 1. Yield strength for a given target ductility ratio vs. structural period

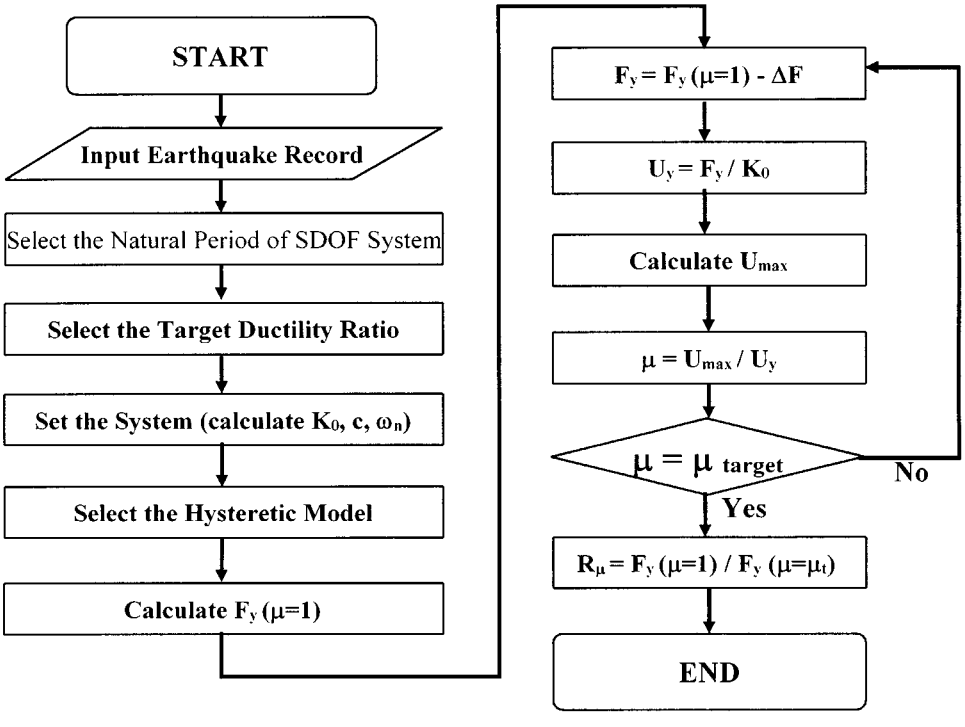

Figure 2. Overall procedure for calibrating the R_μ factor

yield strength decreases. In particular, more than one yield strength corresponding to a given target ductility ratio, μ_t is possible. In this case the largest yield strength is selected in this study since it is more relevant for seismic design.

Ductility ratio, μ is defined as follows:

$$\mu = \frac{\max|u(t)|}{u_y} \tag{2}$$

where $\max|u(t)|$ is the maximum absolute value of relative displacement of the SDOF system with respect to the ground under a given earthquake ground motion, and u_y is the yield displacement of a system.

In order to evaluate the yield strength of an SDOF system for a given target ductility ratio and earthquake ground motion the following equation of motion is used:

$$m\ddot{u}(t) + c\dot{u}(t) + F(t) = -m\ddot{u}_g(t) \tag{3}$$

where m, c and, $F(t)$ are mass, damping factor, and restoring force, respectively, and $u_g(t)$ is ground displacement. Overdots indicate time derivatives.

In this study, the damping ratio is assumed to be 5 per cent of the critical damping for all cases since seismic design provisions are normally based on the 5 per cent damped system.

3. HYSTERETIC MODELS USED IN THIS STUDY

Ductility factor, R_μ, has been evaluated using either the elasto-perfectly plastic or bilinear models because of simplicity. In this study, five different hysteretic models are considered which are (1) elasto-perfectly plastic, (2) bilinear, (3) strength degradation, (4) stiffness degradation, and (5) pinching models. These models are shown in Figure 3. Among these models the elasto-perfectly plastic (EPP) model is used as a basis model in this study. Thus, the effect of other hysteretic models on the R_μ factor is compared with that of the EPP model. The characteristic parameters of each hysteretic model are shown in Table I. The characteristic parameters of each hysteretic model are described by Kunnath *et al.*[8] in detail.

4. EARTHQUAKE RECORDS USED IN THIS STUDY

For the statistical study, 40 earthquake ground motions are used which were obtained from the Earthquake Strong Motion CD-ROM by the National Geographical Data Centre[9] (1996) and the U.S. Geological Survey digital data series, DDS-7, CD-ROM.[7] The software BAP[10] was used for correcting the earthquake records. Also the software SMCAT[11] by the National Geographical Data Centre was used for classifying the earthquake records according to soil type. The soil condition is classified into four types S_1, S_2, S_3, and S_4 according to the Uniform Building Code of 1988.

In this study the ground motions recorded in soil type 1 (S_1) are only considered. According to UBC 1988, solid type 1 (S_1) is classified as 'A soil profile with either (a) a rock-like material characterized by a shear-wave velocity greater than 2500 f/s or by other suitable means of classification, or (b) Stiff or dense soil condition where the soil depth is less than 200 f'. The inventory of selected earthquake records is given in Table II.

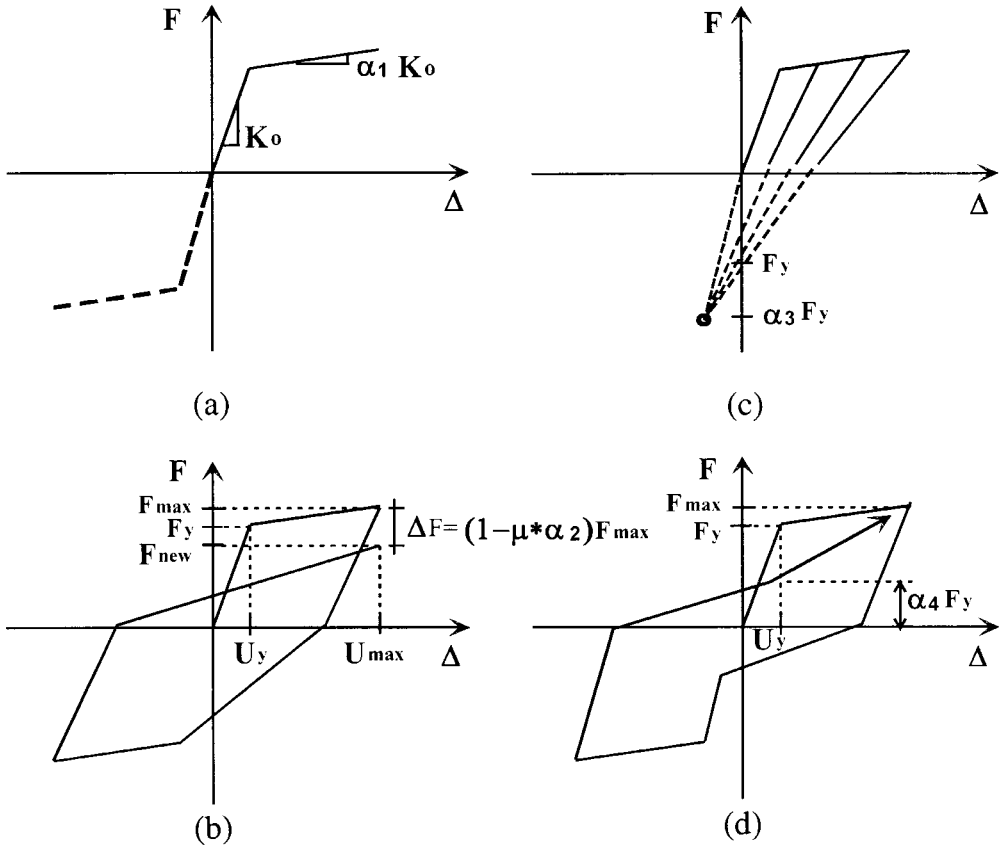

Figure 3. Hysteretic models: (a) bilinear model; (b) strength degradation model; (c) stiffness degradation model; (d) pinching model.

Table I. Key parameters of hysteretic models

Hysteretic model	Parameters	Effect
Elasto-perfectly plastic model	K_0	Initial stiffness
	U_y	Yield displacement
Bilinear model	K_0	Initial stiffness
	U_y	Yield displacement
	α_1	Second slope
Strength degradation model	K_0	Initial stiffness
	U_y	Yield displacement
	α_2	Strength degradation
Stiffness degradation model	K_0	Initial stiffness
	U_y	Yield displacement
	α_3	Stiffness degradation
Pinching model	K_0	Initial stiffness
	U_y	Yield displacement
	α_4	Pinching

Table II. List of earthquake records for S_1 soil site

Event name	Station name	Event data	M	Distance (km)	Component	PGA (cm/s^2)	PGV (cm/s)	PGD (cm)
Offshore Eureka	Cape Mendocino	1994.9.1	7·2	130	90	23·3	2·4	1·5
Western Washington	Olympia, Washington Hwy Test Lab	1949.4.13	7·1	39	356	− 177·8	− 17·8	3·7
Western Washington	Olympia, Washington Hwy Test Lab	1949.4.13	7·0	39	86	274·6	17·0	*
Whittier	Pacoima-Kagel Canyon	1987.10.1	6·1	37	90	154·9	7·7	1·0
Iwate Prefecture	Miyako Harbor Works, Ground	1970.4.1	5·8	17	NS	− 189·7	− 4·4	− 0·3
Iwate Prefecture	Miyako Harbor Works, Ground	1970.4.1	5·8	17	EW	161·8	3·3	− 0·3
Michoacan, Mexico	Calete De Campo	1985.9.19	8·1	20	N90E	137·8	− 12·6	3·2
San Fernando	Lake Hughes, Array Station 4, CA.	1971.2.9	6·5	20	S69E	168·2	5·7	1·2
San Fernando	Lake Hughes, Array Station 4, CA.	1971.2.9	6·5	20	S21W	− 143·5	− 8·6	1·7
Humbolt County	Petrolia, California, Cape Mendocino	1975.6.7	5·3	31	S60E	− 198·7	5·9	0·6
Humbolt County	Petrolia, California, Cape Mendocino	1975.6.7	5·3	31	N30E	103·0	− 3·3	0·4
Kern County	Taft Lincoln School Tunnel	1952.7.21	7·7	42	21	152·7	15·7	*
Kern County	Taft Lincoln School Tunnel	1952.7.21	7·7	42	111	175·9	17·7	*
Puget Sound	Olympia, Washington Hwy Test Lab	1965.4.29	6·5	89	176	194·3	12·7	*
Long Beach	Public Utilities Building	1933.3.10	6·3	29	180	192·7	29·3	*
Long Beach	Public Utilities Building	1933.3.10	6·3	29	270	156·0	15·8	*
Imperial Valley	Holtville P.O.	1979.10.15	6·6	20	225	246·2	44·0	*
Imperial Valley	Calexico Fire Station	1979.10.15	6·6	15	225	269·6	18·2	*
Coalinga	Parkfield Zone 16	1983.5.2	6·5	36	0	178.7	14·7	*

Adak, Alaska, US	Naval Base	1971.5.1	6·8	70	North	85·38	− 3·22	1·40
Alaska Subduction	Cordova, Mt. Eccles School	1964.7.5	5·2	22	N196E	34·20	3·48	0·51
Alaska Subduction	Chernabura Island, 281	1983.2.14	6·3	46	N070E	46·90	3·11	0·34
Alaska Subduction	Chernabura Island, 265	1983.2.14	6·3	48	N070E	16·70	1·05	0·30
Dursunbey	Dursunbey Kandilli Gozlem Istasyonu	1979.7.18	5·2	11	NS	233·77	*	*
Imperial Valley	Cerro Prieto	1979.10.15	6·6	24	135	163·20	*	*
Loma Prieta	Anderson Dam, Left ABT	1989.10.18	7·1	27	250	59·70	12·13	3·77
Mammoth Lakes	Long Valley Dam, L. ABT	1980.5.25	6·1	13	90	− 75·45	7·12	− 3·37
Mammoth Lakes	Long Valleyu Dam, R. Crest	1980.5.25	6·1	13	90	− 147.72	13.06	− 3.89
Mexicali Valley	Cerro Prieto	1979.10.10	4·1	13	S33E	− 42·00	*	*
Miyagi Prefecture	Ofunato Harbor, Jetty	1978.6.12	6·3	103	E41S	− 222·1	14·10	− 5·10
Miyagi Prefecture	Ofunato Harbor, Jetty	1978.6.12	6·3	103	N41E	− 206·70	− 12·8	− 2·20
Morgan Hill	Gilroy-Gavilan College	1984.4.24	6·2	39	67	94·98	− 3·39	0·47
New Ireland	Bato Bridge, Papua New Guinea	1983.3.18	7·7	270	270	31·60	4·12	1·92
San Fernando	800 W. First Street, 1stFl Floor, LA.	1971.2.9	6·5	41	N53W	138·02	19·36	9·99
San Salvador	Hotel Sheraton	1986.10.10	5·4	7	0	213·90	− 17·67	− 4·55
San Salvador	Hotel Sheraton	1986.10.10	5·4	7	270	295·62	26·34	4·36
Sitka, Alaska	Sitka Observatory	1972.7.30	*	86	North	− 70·11	10·79	9·86
West Morland	Superstition Mountain, CA	1981.4.26	5·6	24	135	− 102·47	− 7·67	− 2·03
Whittier Narrows	Garvey Reservoir–Control Building	1987.10.1	5·9	3	330	468·20	19·78	2·21
Whittier Narrows	Griffith Park Observatory	1987.10.1	5·9	22	270	133·80	7·54	0·96

5. DETERMINATION OF DUCTILITY FACTOR, R_μ, CONSIDERING DIFFERENT HYSTERETIC MODELS

It usually requires large computational efforts to calculate the ductility factor. In order to reduce the computational efforts for determining the R_μ factor, this study establishes the functional form of the R_μ factor. According to former research works, [3,12,13,5,6] the R_μ factor is the function of structural period, target ductility, and characteristic parameters of hysteretic models. This study assumes that the R_μ factor is also dependent on these parameters. Thus, the R_μ factor is denoted in the following functional form:

$$R_\mu = f(T, \mu, \alpha_1, \alpha_2, \alpha_3, \alpha_4) \tag{4}$$

The type and parameter of the R_μ function can be obtained by regression analysis. To expedite the regression analysis, the effect of each hysteretic model is assumed to be independent of each other. Thus, equation (4) can be rewritten as follows:

$$R_\mu = R(T, \mu) \times C_{\alpha_1} \times C_{\alpha_2} \times C_{\alpha_3} \times C_{\alpha_4} \tag{5}$$

where $R(T, \mu)$ is the functional format of the R_μ factor of the EPP model which is treated as a basis model in this study. The factors, C_{α_1}, C_{α_2}, C_{α_3}, and C_{α_4}, are considered as correction factors accounting for the effect of bilinear (α_1), strength degradation (α_2), stiffness degradation (α_3), and pinching (α_4) to the R_μ factor obtained from the EPP model.

5.1. The ductility factor, R_μ for elasto-perfectly plastic model

In order to establish the functional form of ductility factor, $R(T, \mu)$ for the EPP model, statistical studies are carried out. The 11 200 R_μ factors are calculated using a non-linear dynamic analysis of the SDOF system considering the following permutations:

(1) Target ductility ratios of 1 (elastic behaviour), 2, 3, 4, 5, 6, and 8 (7).
(2) Forty discrete natural periods of the SDOF systems from 0·05 s to 3·0 s (40),
(3) Forty earthquake ground motions recorded at an S_1 site (40).

Two stage regression analysis is carried out in the two-dimensional domain. In the first stage, the function for R_μ vs. the natural period of SDOF is regressed for the discrete values of ductility ratios, and then the effect of the ductility ratio is evaluated at the second stage. The following function is obtained for the EPP model

$$R_\mu = R(T, \mu) = A_0 \times \{1 - \exp(-B_0 \times T)\} \tag{6}$$

$$A_0 = 0{\cdot}99 \times \mu + 0{\cdot}15 \tag{7}$$

$$B_0 = 23{\cdot}69 \times \mu^{-0{\cdot}83} \tag{8}$$

where T is the natural period and μ is the ductility ratio.

Figure 4 shows the fitness of the regressed function of the R_μ factor. In this figure, the solid line represents the values obtained from the regressed function and the dashed line represents the actual mean values of R_μ factors obtained from 12,800 non-linear dynamic analyses. In Figure 5, the solid lines represent the values obtained from the regressed Equations (7) and (8), and the

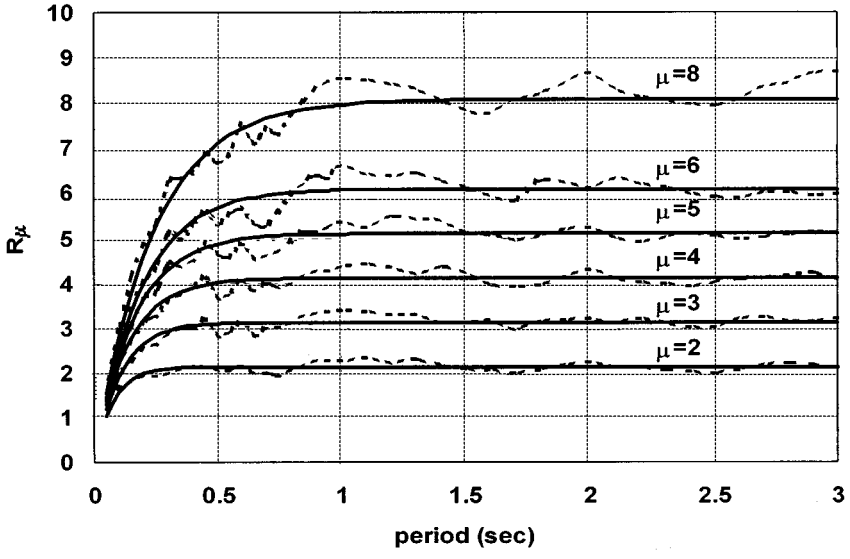

Figure 4. Fitness of the regressed R_μ factor

circle represents the actual values. Also Figure 6 compares the values of the R_μ factors provided by several researchers.

5.2. *The effect of the second slope of the bilinear model*

The characteristic parameter of the bilinear model is α_1, which accounts for the second slope. As mentioned earlier, this study accounts for the effect of the second slope using correction factor, $C_{\alpha 1}$. This correction factor calibrates the ductility factor, R_μ, which is obtained from the EPP model in order to account for the effect of the bilinear model. Figure 7 shows the R_μ factor vs. the structural period with the different levels of the second slope ($\alpha_1 = 0$, 2, 5, 7, 10 and 15 per cent). From this figure, it is found that a larger R_μ factor is obtained as the second slope increases. Table IIIa shows the ratio of the R_μ factor obtained from the bilinear model to that from the EPP elasto-perfectly plastic model for different levels of the second slope and the target ductility ratio. From this table, the correction factor should be a function of both α_1 and μ_t. Based on this finding, the following functional form of correction factor $C_{\alpha 1}$ is obtained using two-stage regression analyses. At the first stage, correction factor $C_{\alpha 1}$ vs. α_1 is regressed for the discrete values of the target ductility ratio and then the effect of the target ductility ratio is evaluated at the second stage. For this regression analysis a total number of 67 200 non-linear dynamic analyses are performed for the number of permutations described in Section 5.1 with six different second slopes. The following regressed function is obtained:

$$R_\mu = R(T, \mu) \times C_{\alpha_1} \tag{9}$$

where

$$C_{\alpha_1} = 1{\cdot}0 + A_1 \times \alpha_1 + B_1 \times \alpha_1^2 \tag{10}$$

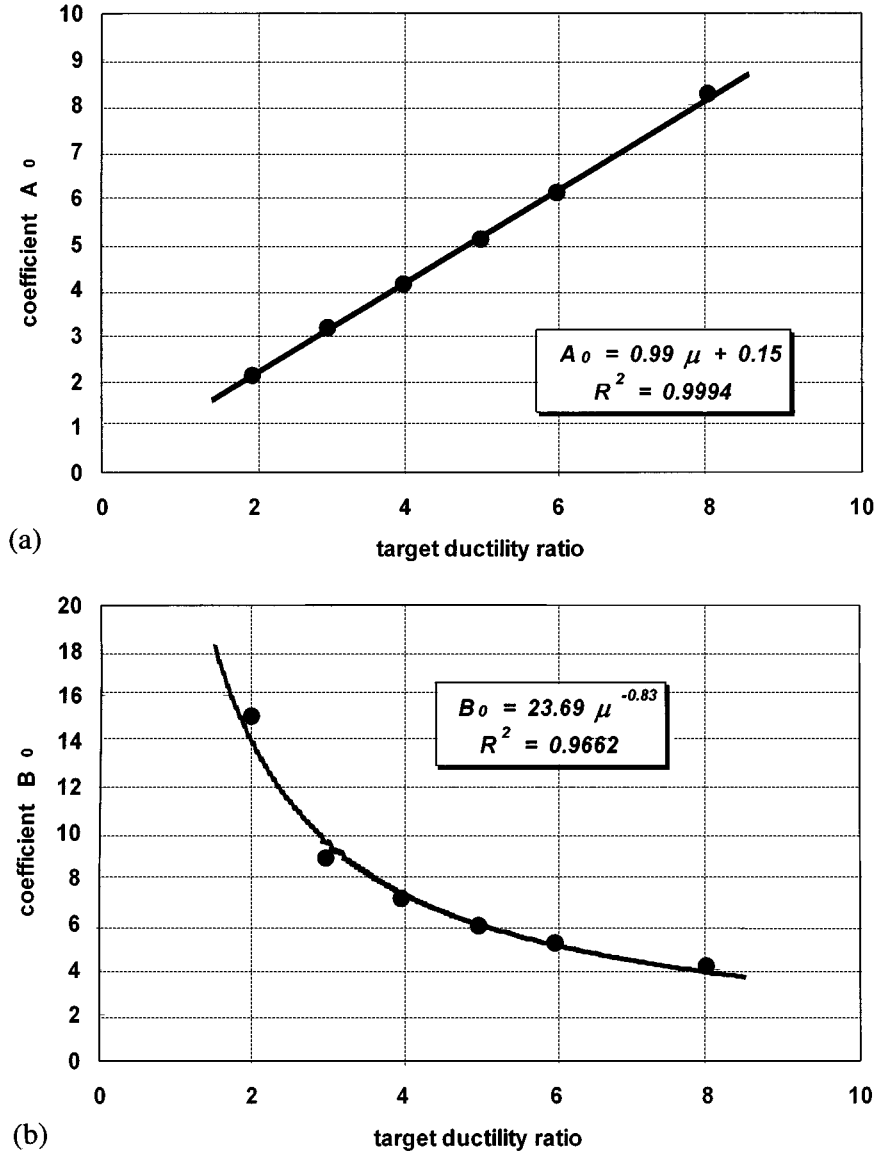

Figure 5. Coefficients of the R_μ factor for the EPP Model: (a) fitness of coefficient A_0; (b) fitness of coefficient B_0.

with

$$A_1 = 2{\cdot}07 \times \ln(\mu) - 0{\cdot}28 \tag{11}$$

and

$$B_1 = -10{\cdot}55 \times \ln(\mu) + 5{\cdot}21 \tag{12}$$

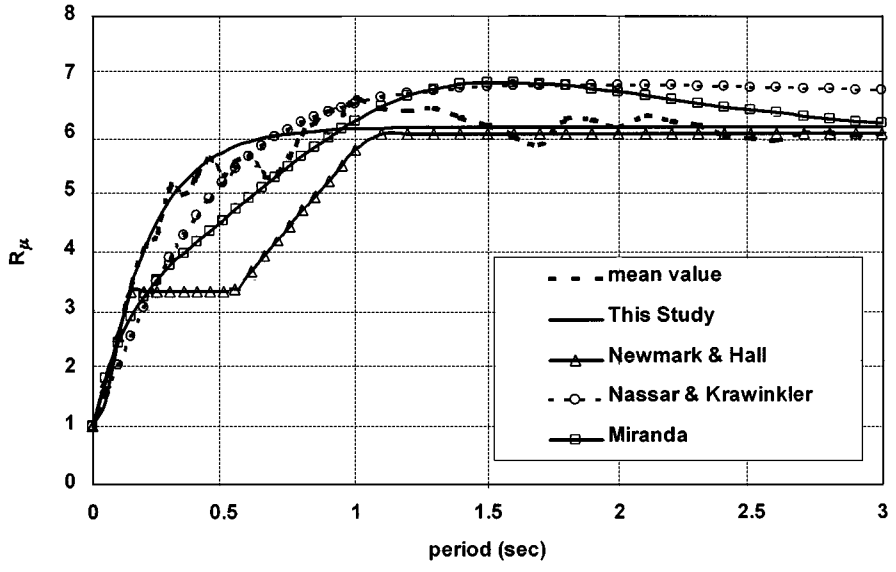

Figure 6. Comparison of R_μ functions ($\mu = 6$)

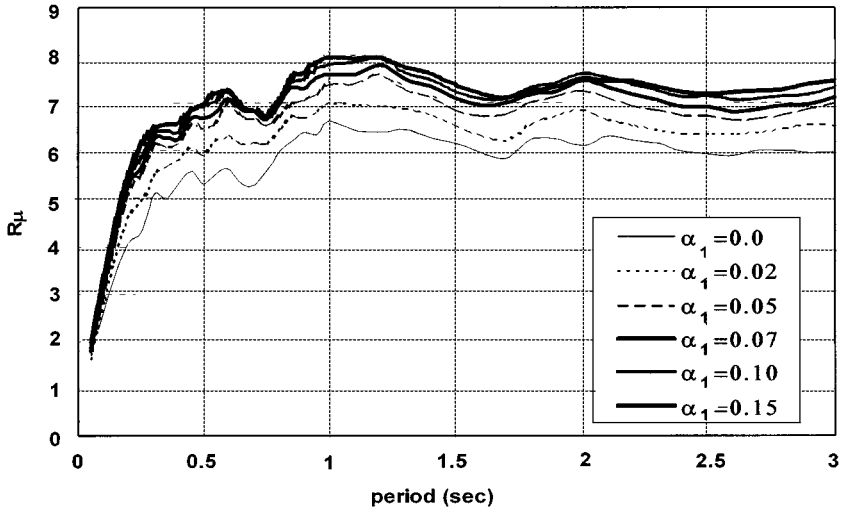

Figure 7. Effect of the second slope on the R_μ factor

Figure 8 shows the fitness of the R_μ factor which can account for the second slope effects to the mean values of R_μ factors. In this figure, the solid line represents the regressed function and the dashed line represents the mean values obtained from non-linear dynamic analyses of the SDOF system.

Table III. Average increment/decrement of R_μ factor due to different hysteretic models

Target ductility	(a) R_μ factor of bilinear model to one of EPP model (percentage)					
	for $\alpha_1 = 0\%$	for $\alpha_1 = 2\%$	for $\alpha_1 = 5\%$	for $\alpha_1 = 7\%$	for $\alpha_1 = 10\%$	for $\alpha_1 = 15\%$
$\mu = 2$	100	103	107	109	112	117
$\mu = 3$	100	104	110	113	116	120
$\mu = 4$	100	105	112	116	119	122
$\mu = 5$	100	106	114	118	122	124
$\mu = 6$	100	107	115	119	123	125
$\mu = 8$	100	108	117	122	126	127
Target ductility	(b) R_μ factor of strength degradation model to one of EPP model (percentage)					
	for $\alpha_2 = 0\%$	for $\alpha_2 = 3\%$	for $\alpha_2 = 6\%$	for $\alpha_2 = 9\%$	for $\alpha_2 = 12\%$	for $\alpha_2 = 15\%$
$\mu = 2$	100	98	96	94	91	89
$\mu = 3$	100	97	94	92	89	87
$\mu = 4$	100	96	93	90	87	84
$\mu = 5$	100	95	91	88	85	82
$\mu = 6$	100	95	91	87	84	80
$\mu = 8$	100	94	89	85	81	77
Target ductility	(c) R_μ factor of stiffness degradation model to one of EPP model (percentage)					
	for $\alpha_3 = 15$	for $\alpha_3 = 4$	for $\alpha_3 = 2$	for $\alpha_3 = 1$	for $\alpha_3 = 0{\cdot}5$	for $\alpha_3 = 0$
$\mu = 2$	100	99	97	94	91	85
$\mu = 3$	100	99	97	94	91	85
$\mu = 4$	100	99	97	94	91	85
$\mu = 5$	100	99	97	94	91	85
$\mu = 6$	100	99	97	94	91	85
$\mu = 8$	100	99	97	94	91	85
Target ductility	(d) R_μ factor of pinching model to one of EPP model (percentage)					
	for $\alpha_4 = 100\%$	for $\alpha_4 = 40\%$	for $\alpha_4 = 30\%$	for $\alpha_4 = 20\%$	for $\alpha_4 = 10\%$	for $\alpha_4 = 5\%$
$\mu = 2$	100	99	98	97	94	92
$\mu = 3$	100	99	98	96	94	92
$\mu = 4$	100	98	97	96	94	92
$\mu = 5$	100	98	97	96	93	92
$\mu = 6$	100	98	97	95	93	92
$\mu = 8$	100	98	96	95	93	92

5.3. The effect of the strength degradation model

Strength degradation may be important for reinforced concrete structures, particularly in the structure with a low shear capacity. In order to establish the functional form of the correction factor accounting for the effect of strength degradation (α_2), two stage regression analysis is also carried out based on 56 000 values of R_μ factors obtained from non-linear dynamic analysis. Six

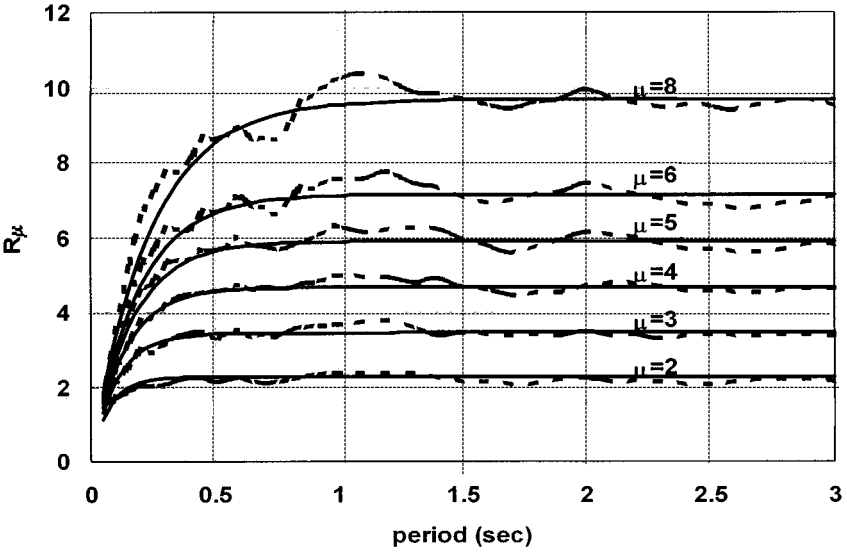

Figure 8. Fitness of the R_μ factor ($\alpha_1 = 7\%$)

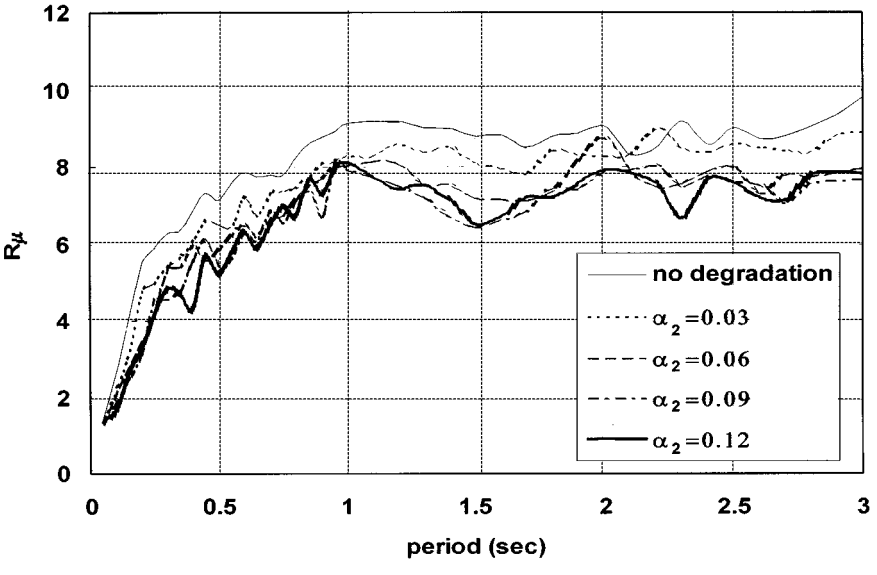

Figure 9. Effect of strength degradation

different levels of strength degradation ($\alpha_2 = 0$, 3, 6, 9, and 12 per cent) are considered. Mean values of the R_μ factor with the different levels of strength degradation are shown in Figure 9. As shown in this figure, the R_μ factor decreases with an increasing level of strength degradation. Also, from Table IIIb, the correction factor should be a function of the target ductility ratio. Based on

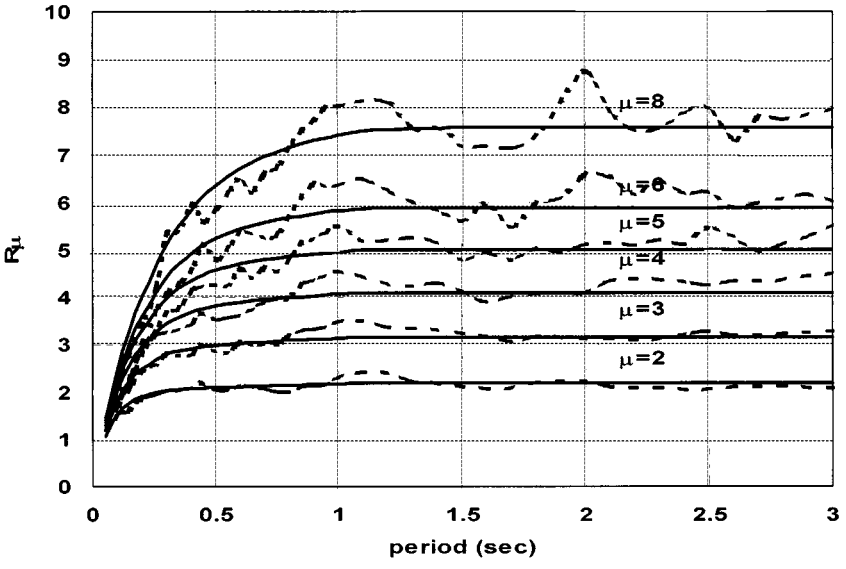

Figure 10. Fitness of the R_μ factor ($\alpha_2 = 6\%$)

this fact, the following functional form of correction factor C_{α_2} is obtained using a procedure similar to that for C_{α_1}.

$$R_\mu = R(T, \mu) \times C_{\alpha_2} \tag{13}$$

where

$$C_{\alpha_2} = \frac{1}{A_2 \times \alpha_2 + B_2} \tag{14}$$

with

$$A_2 = 0{\cdot}2 \times \mu + 0{\cdot}42 \tag{15}$$

and

$$B_2 = 0{\cdot}005 \times \mu + 0{\cdot}98 \tag{16}$$

Figure 10 shows the fitness of the values of the R_μ factor obtained from a regressed function to the actual mean values of the R_μ factor. In this figure, the solid line represents the regressed function and the dashed line denotes the actual values.

5.4. The effect of the stiffness degradation model

Stiffness degradation reduces the energy dissipation capacity of a system. Thus, it is expected that a lower ductility factor is required for the system with stiffness degradation than for the EPP system. Figure 11 shows that a lower ductility factor is obtained as the level of stiffness degradation increases. From Table IIIc, the correction factor C_{α_3} is also a function of the level of stiffness degradation. For statistical analysis, 67 200 R_μ factors are obtained using non-linear

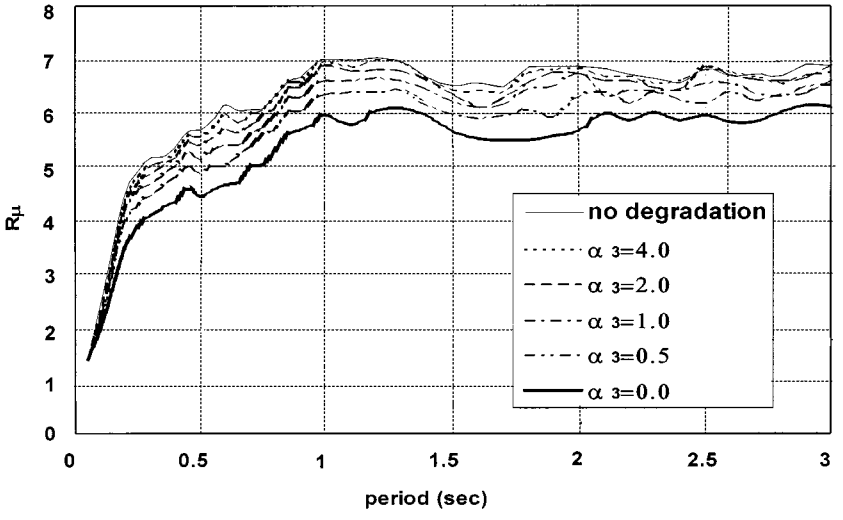

Figure 11. Effect of stiffness degradation

dynamic analyses of the SDOF system. Six different levels of stiffness degradation ($\alpha_3 = 15, 4, 2, 1, 0{\cdot}5$ and 0) are considered. Two-stage regression analysis is also used to establish the functional form of C_{α_3}. The following function is obtained:

$$R_\mu = R(T, \mu) \times C_{\alpha_3} \tag{17}$$

where

$$C_{\alpha_3} = \frac{0{\cdot}85 + B_3 \times \alpha_3}{1 + C_3 \times \alpha_3 + 0{\cdot}001 \times \alpha_3^2} \tag{18}$$

with

$$B_3 = 0{\cdot}03 \times \mu + 1{\cdot}02 \tag{19}$$

and

$$C_3 = 0{\cdot}03 \times \mu + 0{\cdot}99 \tag{20}$$

Figure 12 shows the fitness of the R_μ factor. In this figure, the solid line represents the regressed function and the dashed line represents the real mean values of the R_μ factor.

5.5. The effect of the pinching model

The presence of open cracks in the compression zone of reinforced concrete members causes a marked pinching of its hysteretic behaviour. Pinching narrows the hysteresis loops so that the energy dissipation capacity of a member or system becomes lower due to pinching as shown in

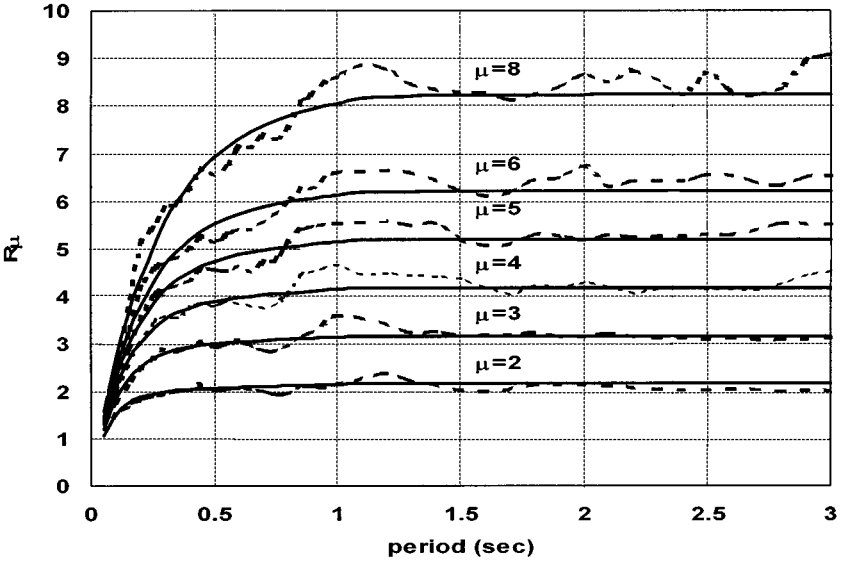

Figure 12. Fitness of the R_μ factor ($\alpha_3 = 1.0$)

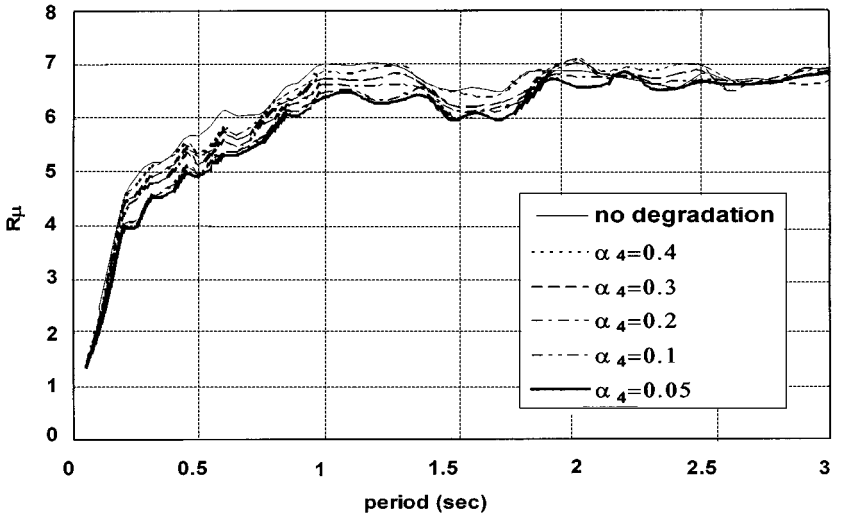

Figure 13. Effect of pinching

Figure 13. As the level of pinching becomes higher, the R_μ factor is expected to be lower. The correction factor, C_{α_4} accounts for the effect of pinching. For regression analysis to establish the functional form of C_{α_4}, 67 200 values of R_μ factors are calculated using non-linear dynamic analyses with 6 different levels of pinching ($\alpha_4 = 1{\cdot}0$, $0{\cdot}4$, $0{\cdot}3$, $0{\cdot}2$, $0{\cdot}1$ and $0{\cdot}05$). From Table IIId,

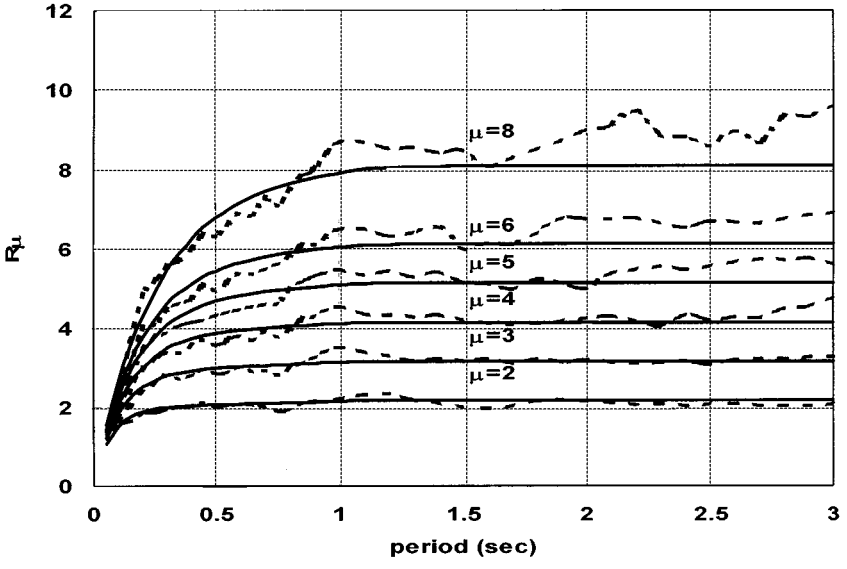

Figure 14. Fitness of the R_μ factor ($\alpha_4 = 0{\cdot}1$)

the factor C_{α_4} is a function of the level of pinching and target ductility ratio. Following the functional form of C_{α_3}, the C_{α_4} factor is obtained using two-stage regression analysis.

$$R_\mu = R(T, \mu) \times C_{\alpha_4} \tag{21}$$

where

$$C_{\alpha_4} = \frac{1}{1 + 0{\cdot}11 \times \exp(-C_{\alpha_4} \times \alpha_4)} \tag{22}$$

with

$$C_4 = -1{\cdot}4 \times \ln(\mu) + 6{\cdot}6 \tag{23}$$

Figure 14 shows the fitness of the R_μ factor which accounts for the pinching effects to the mean value of R_μ factors. In this figure, the solid line denotes the regressed function and the dashed line denotes the actual mean values of the R_μ factor.

5.6. Validity of proposed R_μ function for the system having combined hysteretic characteristics

The functional form of the R_μ factor established in this study is examined using several systems with combined hysteretic characteristics (e.g. the system with bilinear, and strength degradation). Figure 15 shows the fitness of R_μ factor obtained from the regressed function to the actual R_μ factor for two systems having combined hysteretic characteristics.

This figure shows that the functional form of the R_μ factor fits the actual R_μ values with good precision. Therefore, the functional forms proposed in this study could be used to calculated the

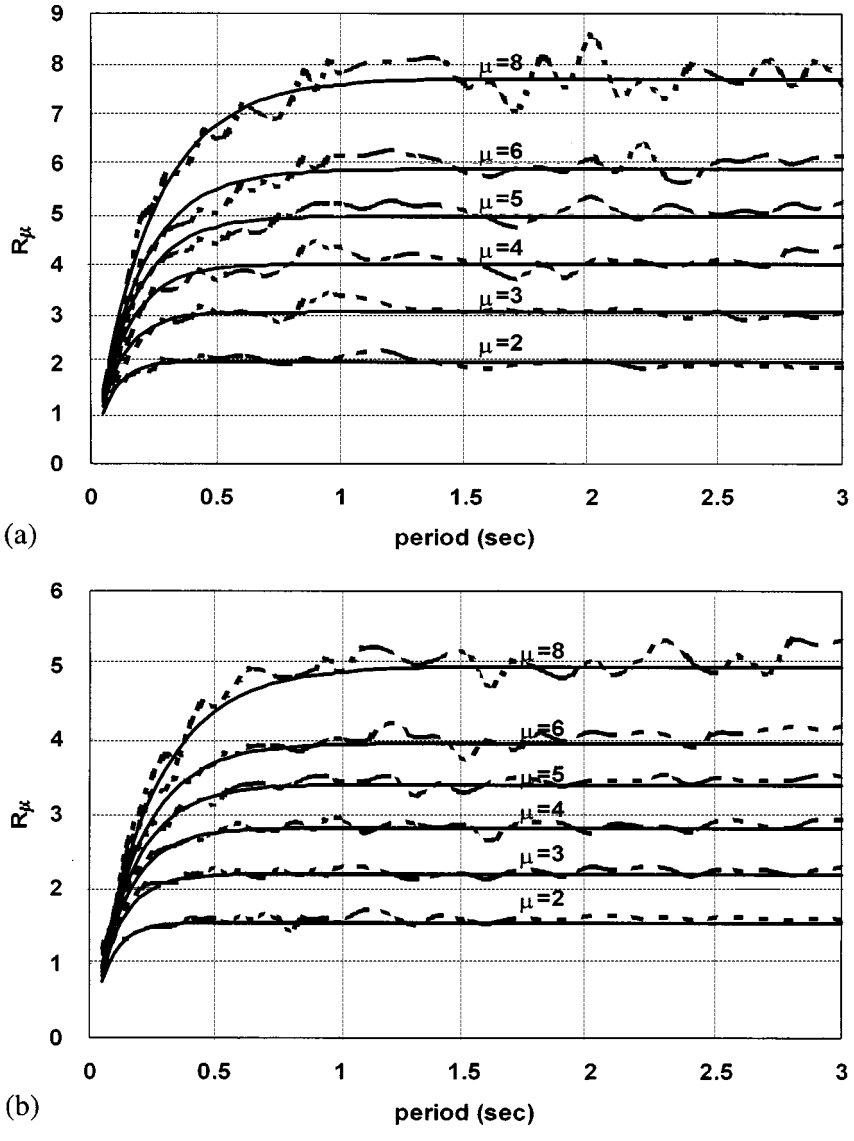

Figure 15. Fitness of the R_μ factor: (a) for $\alpha_1 = 5\%$, $\alpha_2 = 6\%$, $\alpha_3 = 2{\cdot}0$, $\alpha_4 = 30\%$; (b) for $\alpha_1 = 0\%$, $\alpha_2 = 12\%$, $\alpha_3 = 0{\cdot}0$, $\alpha_4 = 5\%$

R_μ factor. The difference between actual and predicted values of the R_μ factor is tested using residual. In this study, residual (e) is defined as

$$e = \frac{1}{n}\sum_{i=1}^{n}\left|\frac{R_\mu - R_{\text{actual}}}{R_{\text{actual}}}\right| \times 100(\%) \tag{24}$$

Table IV. Evaluation of average residual between actual and predicted R_μ factors

Target ductility	Average residual to actual R_μ factor (percentage)			
	for $\alpha_1 = 7\%$, $\alpha_2 = 3\%$, $\alpha_3 = 1{\cdot}0\%$, $\alpha_4 = 10\%$,	for $\alpha_1 = 5\%$, $\alpha_2 = 6\%$, $\alpha_3 = 2{\cdot}0\%$, $\alpha_4 = 30\%$,	for $\alpha_1 = 0\%$, $\alpha_2 = 9\%$, $\alpha_3 = 4{\cdot}0\%$, $\alpha_4 = 40\%$,	for $\alpha_1 = 0\%$, $\alpha_2 = 12\%$, $\alpha_3 = 0{\cdot}0\%$, $\alpha_4 = 5\%$,
$\mu = 2$	3·3	3·9	3·6	4·8
$\mu = 3$	3·2	3·8	3·9	3·5
$\mu = 4$	3·0	4·3	3·6	3·9
$\mu = 5$	2·7	3·7	3·4	3·0
$\mu = 6$	3·0	4·0	3·3	3·8
$\mu = 8$	3·2	3·8	4·5	3·9

Table IV shows the average residual of R_μ factor for different target ductility ratios. The average residual varies within 2·7 to 4·8 per cent of the actual R_μ factor. The target ductility ratio gives a small effect on the variation of average residual.

6. CONCLUSION

Strength reduction factor (ductility factor), R_μ, is defined as the ratio of elastic strength demand imposed on the SDOF system to inelastic strength demand for a given ductility ratio. The main objective of this study is to evaluate the R_μ factor which accounts for the effect of different hysteretic models. This study considers the soil profile with stiff soil or rock (classified as S_1 in UBC). Statistical studies are carried out to establish the functional form of the R_μ factor. According to the results of this study, the following conclusions are made:

1. For a given target ductility ratio, the ductility factor R_μ is strongly dependent on the change of the period, particularly in the short-period range.
2. As the level of the second slope of a bilinear system is higher, the value of the ductility factor R_μ becomes greater. Thus, the effect of the second slope needs to be accounted for when the R_μ factor is evaluated.
3. According to the results of this study, the R_μ factor is affected by the level of strength degradation, stiffness degradation, and pinching. A lower R_μ factor is obtained with an increase of the level of stiffness and strength degradation, and pinching. Therefore, it is concluded that the effects of these hysteretic characteristics should be accounted properly for evaluating the R_μ factor.
4. This study assumes that the effect of each hysteretic model on the R_μ factor is independent of those of other hysteretic models. Figure 15 and Table IV show that this assumption is valid. Therefore, the proposed functional form can be used to calculate the R_μ factor of a system having combined hysteretic characteristics such as bilinear, strength degradation, stiffness degradation, and pinching.
5. According to the results of this study, the ductility factor, R_μ is a function of the structural period, and the level of the target ductility ratio, second slope, strength degradation, stiffness

degradation, and pinching. The following proposed R_μ functions can account for these effects explicitly:

$$R_\mu = R(T,\mu) \times C_{\alpha_1} \times C_{\alpha_2} \times C_{\alpha_3} \times C_{\alpha_4}$$

$$R(T,\mu) = A_0 \times \{1 - \exp(-B_0 \times T)\}, \quad A_0 = 0{\cdot}99 \times \mu + 0{\cdot}15, \quad B_0 = 23{\cdot}69 \times \mu^{-0{\cdot}83}$$

$$C_{\alpha_1} = 1{\cdot}0 + A_1 \times \alpha_1 + B_1 \times \alpha_1^2, \quad A_1 = 2{\cdot}07 \times \ln(\mu) - 0{\cdot}28, \quad B_1 = -10{\cdot}55 \times \ln(\mu) + 5{\cdot}21$$

$$C_{\alpha_2} = \frac{1}{A_2 \times \alpha_2 + B_2}, \quad A_2 = 0{\cdot}2 \times \mu + 0{\cdot}42, \quad B_2 = 0{\cdot}005 \times \mu + 0{\cdot}98$$

$$C_{\alpha_3} = \frac{0{\cdot}85 + B_3 \times \alpha_3}{1 + C_3 \times \alpha_3 + 0{\cdot}001 \times \alpha_3^2}, \quad B_3 = 0{\cdot}03 \times \mu + 1{\cdot}02, \quad C_3 = 0{\cdot}03 \times \mu + 0{\cdot}99$$

$$C_{\alpha_4} = \frac{1}{1 + 0{\cdot}11 \times \exp(-C_4 \times \alpha_4)}, \quad C_4 = -1{\cdot}4 \times \ln(\mu) + 6{\cdot}6$$

where $R(T,\mu)$ is the functional form of the R_μ factor for the EPP model, and the factors, C_{α_1}, C_{α_2}, C_{α_3} and C_{α_4} are correction factors which account for the effect of bilinear(α_1), strength degradation(α_2), stiffness degradation(α_3), and pinching(α_4), respectively.

6. In this study, the damping is assumed to be of viscous type with a fixed damping coefficient. Therefore, further study is needed to examine other damping characteristics such as instantaneous stiffness proportional damping. Also, this study only considers SDOF systems. The R_μ factor for MDOF systems has to be studied systematically.

ACKNOWLEDGEMENTS

This research was supported by Engineering Research Center for Advanced Structure Research Station (STRESS) of KOSEF at Hanyang University.

REFERENCES

1. ATC, 'A critical review of current approaches to earthquake-resistant design', *Applied Technology Council Report ATC-34*, Redwood City, California, 1995.
2. ATC, 'Structural response modification factors', *Applied Technology Council Report ATC-19*, Redwood City, California, 1995.
3. N. M. Newmark and W. J. Hall, 'Procedures and criteria for earthquake resistant design', *Building Research Series No. 46*, National Bureau of Standards, U.S. Dept. of Commerce, Washington, 1973, pp. 209–236.
4. R. Riddell and N. M. Newmark, 'Statistical analysis of the response of nonlinear systems subjected to earthquakes', *Structural Research Series No. 468,* Department of Civil Engineering, University of Illinois, Urbana, 1979.
5. A. A. Nassar and H. Krawinkler, 'Seismic demands for SDOF and MDOF systems', *John A. Blume Earthquake Engineering Center Report No. 95*, Stanford University, CA, 1991.
6. E. Miranda, 'Site-dependent strength reduction factors', *J. Struct. Engng.* **119**, 3503–3519 (1993).
7. S. W. Han and Y. K. Wen, 'Methods of reliability-based seismic design I: equivalent nonlinear system', *J. Struct. Engng.* **123**, 256–263 (1997).
8. S. K. Kunnath, A. M. Reinhorn and Y. J. Park, 'Analytical modeling of inelastic seismic response of R/C structures', *J. Struct. Engng.* **116**, 996–1017 (1990).
9. NGDC, 'Earthquake strong motion CD-ROM collection', *Product No. 1145-A27-001*, National Geographical Data Center, Boulder, CO, 1989.
10. BAP, 'Basic strong-motion accelerogram processing software version 1.0', *Open File Report 92-296A*, US Geological Survey, 1992.

11. SMCAT, *An Earthquake Strong Motion Data Catalog for Personal Computers*, National Geographical Data Center, Boulder, CO, 1989.
12. S. W. Han and Y. K. Wen, 'Methods of reliability-based seismic design II: calibration of design parameters', *J. Struct. Engng.* **123**, 264–270 (1997).
13. J. D. Osteraas and H. Krawinkler, 'Strength and ductility considerations in seismic design', *John A. Blume Earthquake Engineering Center Report No. 90*, Stanford Univ., CA, 1990.
14. H. Krawinkler, 'New trends in seismic design methodology', *Proc. of 10th European Conf. Earthquake Engng.*, Duma, 1995, pp. 821–830.
15. L. C. Seekins, A. G. Brady, C. Carpenter and N. Brown, 'Digitized strong-motion accelerograms of North and Central American earthquake 1933–1986', *Digital Data Series DDS-7*, US Geological Survey, 1992.
16. Y. H. Oh, S. W. Han and L. H. Lee, 'Effect of post-yielding stiffness on the ductility dependent strength reduction factor', *J. Architect. Inst. Korea* AIK **114**, 353–360 (1988).

